STEM CELLS®

CANCER STEM CELLS

Reciprocal Reprogramming of Cancer Cells and Associated Mesenchymal Stem Cells in Gastric Cancer

YEELA SHAMAI,[a] DALIA COHN ALPEROVICH,[c] ZOHAR YAKHINI,[c,d] KARL SKORECKI,[a,b,e] MATY TZUKERMAN[a,b]

Key Words. Tumor microenvironment • Tumor associated MSC • Reprogramming of MSC • Tumor-stromal cell interactions • Cancer stem cells • Organotypic culture • Gastric cancer

[a]Rambam Medical Center, Haifa, Israel; [b]Rappaport Faculty of Medicine and Research Institute, Haifa, Israel; [c]Computer Science Department, Technion-Israel Institute of Technology, Haifa, Israel; [d]Arazi School of Computer Science, Interdisciplinary Center, Herzliya, Israel; [e]Technion-Israel Institute of Technology, Haifa, Israel

Correspondence: Maty Tzukerman, Ph.D., Molecular Medicine Laboratory, B. Rappaport Faculty of Medicine, Technion-Israel Institute of Technology, P.O.B. 9649, Bat Galim, Haifa 31096, Israel. Telephone: 972-4-8295277/81; e-mail: bimaty@techunix.technion.ac.il

Received April 4, 2018; accepted for publication October 16, 2018; first published online in STEM CELLS *EXPRESS* October 31, 2018.

http://dx.doi.org/10.1002/stem.2942

ABSTRACT

The interactions of cancer stem cells (CSCs) within the tumor microenvironment (TME), contribute to the overall phenomenon of intratumoral heterogeneity, which also involve CSC interactions with noncancer stromal cells. Comprehensive understanding of the tumorigenesis process requires elucidating the coordinated gene expression between cancer and tumor stromal cells for each tumor. We show that human gastric cancer cells (GSC1) subvert gene expression and cytokine production by mesenchymal stem cells (GSC-MSC), thus promoting tumor progression. Using mixed composition of human tumor xenografts, organotypic culture, and in vitro assays, we demonstrate GSC1-mediated specific reprogramming of "naïve" MSC into specialized tumor associated MSC equipped with a tumor-promoting phenotype. Although paracrine effect of GSC-MSC or primed-MSC is sufficient to enable 2D growth of GSC1, cell–cell interaction with GSC-MSC is necessary for 3D growth and in vivo tumor formation. At both the transcriptional and at the protein level, RNA-Seq and proteome analyses, respectively, revealed increased R-spondin expression in primed-MSC, and paracrine and juxtacrine mediated elevation of Lgr5 expression in GSC1, suggesting GSC-MSC-mediated support of cancer *stemness* in GSC1. CSC properties are sustained in vivo through the interplay between GSC1 and GSC-MSC, activating the R-spondin/Lgr5 axis and WNT/β-catenin signaling pathway. β-Catenin+ cell clusters show β-catenin nuclear localization, indicating the activation of the WNT/β-catenin signaling pathway in these cells. The β-catenin+ cluster of cells overlap the Lgr5+ cells, however, not all Lgr5+ cells express β-catenin. A predominant means to sustain the CSC contribution to tumor progression appears to be subversion of MSC in the TME by cancer cells. STEM CELLS *2019;37:176–189*

SIGNIFICANCE STATEMENT

This article describes the utilization of patient gastric carcinoma-derived cancer cells (GSC1) to demonstrate subversion of naïve MSC from adjacent tissue, which are reprogrammed to express a tumor-promoting phenotype, whose cardinal manifestation is to sustain CSC. Paracrine effects of such primed-MSC are sufficient to enable 2D growth of GSC1, while cell–cell interactions are necessary for 3D growth or in vivo tumor formation. Increased expression of R-spondin in primed-MSC mediated elevation of Lgr5 expression in GSC1, activation of the WNT/β-catenin signaling pathway and β-catenin nuclear translocation. Subversion of MSC by cancer cells appears to be a prominent means to sustain the CSC underpinning of tumor progression.

INTRODUCTION

Recruitment of tumor supporting stromal cells coupled with extensive remodeling of adjacent tissues are essential for providing a tumor microenvironment (TME) which supports cancer cell proliferation, invasion, metastasis, and chemoresistance [1–7]. Tumor-supporting stromal cells include cancer associated fibroblasts, mesenchymal stem cells (MSC), endothelial cells, and immune cells that interact both with the tumor cells, as well as with each other to drive tumor progression and drug resistance. However, despite accumulating evidence for stromal effects on cancer cells, little is known about the transcriptional regulators that are responsible for tumor-supporting stromal reprogramming, more specifically with respect to MSC in the tumor stroma.

MSC are recruited by the cancer cells into the tumor site from either the bone marrow or

from adjacent tissues, and become an integral cellular component of the TME where they modulate tumor progression [8–11]. MSC tropism into tumor sites is mediated by a combination of extrinsic signals together with secretion of chemokines, cytokines and growth factors secreted by cells of the TME [3–7]. The intercellular communication among tumor cancer cells and recruited MSC can be executed either through cell-to-cell contact, or through paracrine interactions mediated by secreted signaling molecules and/or through microvesicles (MV) constitutively shed from cancer cells and MSC [4, 5, 7, 12–14].

A single tumor mass comprises heterogeneous cancer cell populations, each displaying diverse cellular morphology, phenotypic expression, tumor initiation capacities and inherent or acquired resistance to anticancer drugs. This complex intratumoral heterogeneity contributes to the "nefarious ingenuity" of human cancers and challenges their eradication. Accumulating evidence shows that both the "cancer stem cells" (CSCs) and the "clonal evolution" models, can explain the intratumoral heterogeneity, as CSCs undergo clonal evolution [15–22]. The continuous accumulation of mutations generates heterogeneity of cells within a solid tumor and its metastases, causing certain subsets of tumor cells become more aggressive during tumor progression. A crucial insight relates to understanding that the self-renewal capacity of CSC is not a durable state, but rather a dynamic and niche-dependent process [18, 19]. Tumor stroma interaction signals also regulate epithelial cancer cell plasticity via epithelial to mesenchymal transition programs. This facilitates invasion and metastasis of cancer cells, enables non-CSCs to convert into CSCs, and may influence the TME by converting cancer cells into tumor supportive stroma [23–26]. The complexity and plasticity of solid tumors is enabled by a TME that provides a compatible network of interactions between the heterogeneous cancer cells and non-neoplastic tumor-supporting cells [19, 27–29]. Therefore, attempts to eradicate a single stable self-renewing subpopulation within any given tumor are often futile.

In gastric carcinoma, malignant cells reside within a TME niche comprised of a rich milieu of different types of stromal cells and ECM which contribute to tumorigenesis and resistance to therapy [3, 30]. Several studies have described various roles of the TME, but none have investigated its relevance to clinical drug responsiveness [31–33]. In addition, these and other studies have led to important advances in characterization of gastric CSC subpopulations with properties of self-renewal, sphere forming, drug resistance and in vivo tumorigenicity, which are able to drive tumor growth, recurrence, and metastasis. Gastric CSC express CD44, CD133, CD24, EpCAM, Lgr5, OCT4, Nanog, Sox2, ABCG2, and ALDH1 [34–37].

We have previously reported that the proliferation capacity in vitro and tumorigenesis in vivo of gastric cancer cells (GSC1) extracted from a patient gastric carcinoma, critically depends on the presence of their counterpart GSC-MSC or conditioned medium (CM) derived therefrom [38]. GSC1 cancer cell growth and migration are mediated through activation of the hepatic growth factor (HGF)/c-MET signaling pathway by HGF secreted exclusively from the GSC-MSC. Accordingly, our previous observation revealed the following: (a) HGF levels secreted by GSC-MSC are elevated in the presence of GSC1 CM; (b) significantly increased tumor volume and recapitulation of the original patient tumor phenotype in vivo were observed only when GSC1 cancer cells were injected to SCID/Beige mice together with GSC-MSC; (c) GSC-MSC express extremely high levels of the ABCB1 transporter, which is responsible for decreased drug accumulation in multidrug-resistant cells; and (d) GSC1 cancer cells specifically recruit MSC, which in turn are programmed to secrete HGF [38, 39].

In the current study, we used this experimental platform to examine the alterations in MSC gene expression following in vivo reprogramming by the GSC1 carcinoma cells, which in turn, are potentially available to confer and sustain *stemness* properties in this malignancy.

Materials and Methods

Primary Culture of Cells Derived from Patient Tumor Tissues

Anonymous patient tumor tissue samples were obtained from the Pathology Department of the Rambam Medical Center in accordance with Institutional ethics Review Board (IRB) approval (IRB approval 920110624). The tissue samples were processed to achieve single cell suspensions as described in [38]. Tumor-derived cells were separated into GSC1 cancer cells and GSC-MSC stromal cells which were identified as MSC [38]. Cells were grown in Roswell Park Memorial Institute (RPMI) 1640 medium supplemented with 20% fetal bovine serum, 1% penicillin, and streptomycin. Cell cultures were repeatedly initiated from frozen stocks every 3–4 months, so that the cells durably and consistently maintain the "bona fide" gastric cancer characteristics and xenograft tumor histological phenotype.

Mice and Tumor Formation

Severe combined immune deficiency (SCID)/beige were purchased from Harlan Laboratories Ltd., Jerusalem, Israel. The mice were housed and maintained under specific pathogen-free conditions according to the instructions of the Committee for Oversight of Animal Experimentation at the Technion—Israel Institute of Technology, Haifa, Israel. This was approved by the Institutional Animal Care and Use Committee of the Technion (Protocol #IL-0550516). For tumor formation, 4×10^6 cancer cells were injected into the mice hindlimb musculature and harvested at 60–64 days following injection. Mice were examined for tumor formation once a week and sacrificed by CO_2 inhalation.

In Vivo Reprogramming of MSC

T-MSC were coinjected with GSC1 into the hindlimb musculature of immunodeficient mice. Tumors were harvested, and dissociated into a single cell suspension, as described in detail in Supporting Information [38]. The epithelial cancer cells were separated using human anti-CD326 (EpCAM) microbeads and the fibroblast-like stromal cells were separated using human antifibroblast microbeads with magnetic activated cell sorting. The human origin of the stromal cells was identified using the antihuman mitochondria antibody. The stromal cells were also identified as MSC by flow cytometry positive expression of CD73, CD105, CD90, CD44, and CD29, and negative expression of the hematopoietic stem cell markers CD45, and endothelial progenitor cell marker CD34 as described in detail in Supporting Information. Supporting Information includes additional detailed materials and methods.

RESULTS

Reprogramming of "Naïve" MSC by GSC1 Cancer Cells

In a recent publication [38], we described the synergistic relationship between GSC1 cancer cells and GSC-MSC which may be stronger in some cancers than others, but can fundamentally affect both tumor growth and treatment and should be an important focus for cancer research. To understand the mechanisms underlying the synergistic relationship between GSC1 cancer cells and GSC-MSC tumor stromal cells, we developed an in vivo recruitment/reprogramming process as described in Figure 1A. As previously described for this experimental model [38], we injected GSC1 cancer cells-derived MV encapsulated within matrigel plug, into human embryonic stem cell-derived teratomas generated within immunodeficient mice. MSC recruited from the teratoma tissue into the matrigel plug were extracted, identified as MSC of human origin, and designated as teratoma-derived MSC (T-MSC) that were specifically recruited by GSC1 cancer cells. These GSC1-tropic T-MSC are normal "naïve" cells with a limited population

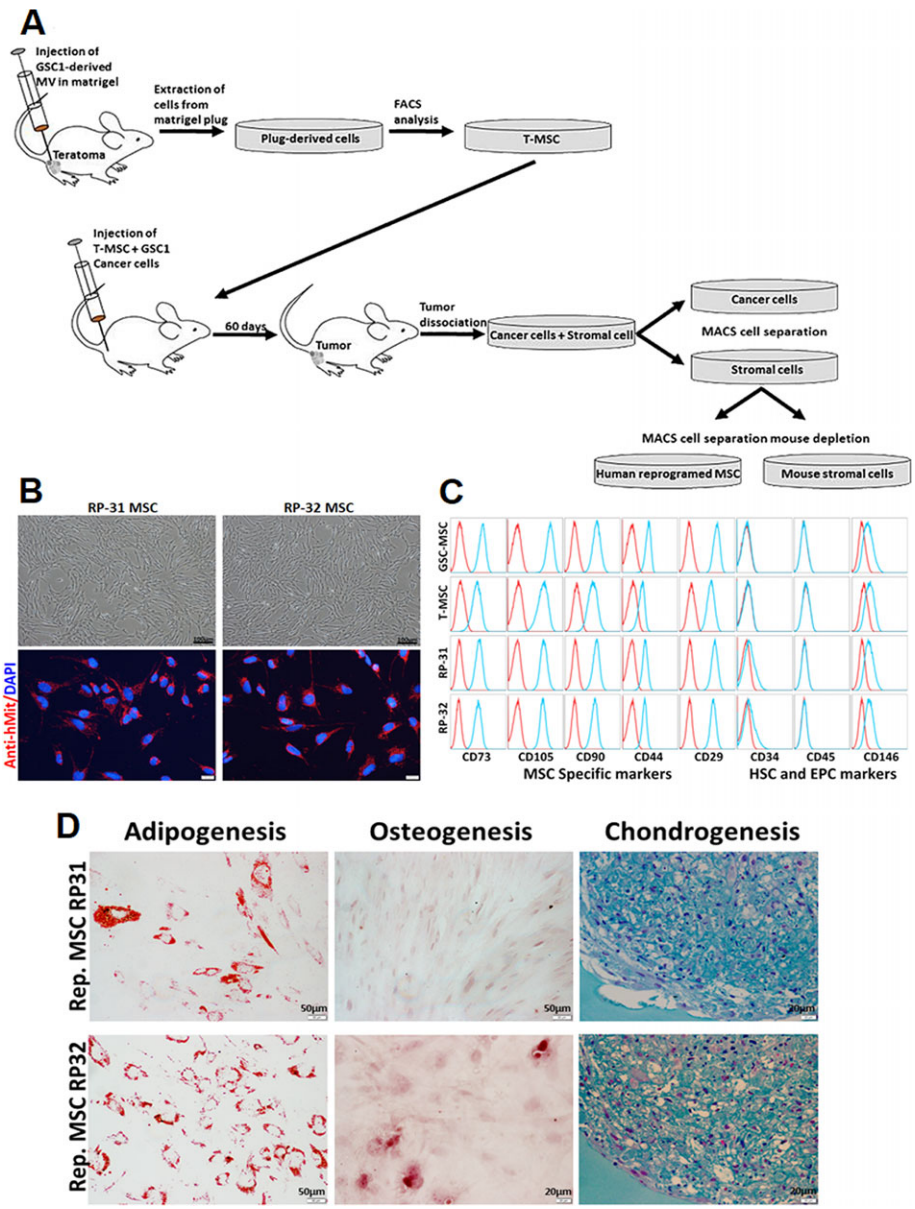

Figure 1. MSC recruitment and reprogramming by gastric cancer cell (GSC1) cancer cells. **(A):** Schematic presentation of the recruitment and reprogramming process. **(B):** Stromal cells extracted from tumors generated by coinjection of GSC1 cells and T-mesenchymal stem cell (MSC) were examined for phenotype (upper panel; scale bars = 100 µm) and for their human origin using antihuman mitochondria (hMit) antibody (lower panel; scale bars = 20 µm). **(C):** The expression of MSC specific cell surface markers in RP-31 and RP-32 MSC in comparison with GSC-MSC and recruited T-MSC, was examined by flow cytometry analysis using a triple staining reaction where CD73 BV421 antibody was used as a reference in each reaction. Red graphs indicate unstained cells. Blue graphs indicate the percentage of cells expressing each specific cell surface antigen. **(D):** The Reprogrammed (RP) MSC RP-31 and RP-32 display a multipotent differentiation capacity into adipocytes, osteoblasts, and chondrocytes (scale bars = 50 µm for adipogenesis, 20 µm for chondrogenesis, 50 µm and 20 µm for osteogenesis of RP-31 and RP-32, respectively).

doubling capacity that were attracted into the matrigel plugs by the GSC1-derived MV and had no prior direct interaction with GSC1 cancer cells [38]. For the reprogramming process, T-MSC were coinjected with GSC1 into the hindlimb musculature of immunodeficient mice as described in Figure 1A. Tumors were harvested and processed as described in [38]. The stromal cells of human origin were identified as MSC by their differentiation capacity and by flow cytometry using previously demonstrated MSC biomarkers [38, 40] (Fig. 1B, 1D). This procedure yielded three different types of MSC: (a) GSC-MSC which are the original patient tumor-derived stromal cells; (b) T-MSC which are "naïve" teratoma-derived MSC specifically recruited by GSC1; and (c) reprogrammed (RP) MSC, RP-31 and RP-32 which were primed by GSC1 cancer cells. Notably, all three types of MSC express the CD146—melanoma cell adhesion molecule on the cell surface which is associated with multipotency [41].

GSC1 Cancer Cell Growth Is Supported by RP MSC In Vitro

The capacity of medium conditioned by the various types of MSC to support the growth of GSC1 in vitro, was examined using the cell proliferation assay. Greater GSC1 proliferation capacity was observed when the cells were grown in GSC-MSC CM as compared with T-MSC CM. However, following reprogramming, GSC1 growth support by RP-31 and RP-32 reprogrammed MSC CM was elevated to the level of GSC-MSC CM (Fig. 2A). Since GSC-MSC elicit their effect on GSC1 growth capacity through a paracrine effect, specifically by secreted HGF [38], we examined whether priming of T-MSC by GSC1 results in increased HGF expression and secretion levels. qRT-PCR analysis, showed increased HGF expression levels in RP-31, RP-32 reprogrammed MSC as compared with the low level of HGF expressed in "naïve" T-MSC (Fig. 2B). As shown in Figure 2C, recruited "naïve" T-MSC secreted low levels of HGF, as previously reported [38]. However, following in vivo priming of T-MSC by GSC1 cancer cells, the HGF secretion level was markedly elevated to levels equivalent those of GSC-MSC. In addition, the levels of HGF encapsulated within MVs derived from "naïve" T-MSC before and after in vivo priming with GSC1 cancer cells was markedly elevated in MV derived from RP-31 and RP-32 reprogrammed MSC (Fig. 2D).

RP MSC Support the Growth of GSC1 Cancer Cells In Vivo

Previous in vivo tumorigenic analyses reported that significantly higher tumor volumes were observed when GSC1 cancer cells were grown in GSC-MSC CM and coinjected with their tumor specific GSC-MSC [38]. Therefore, GSC1 were coinjected with "naïve" T-MSC or with RP-31 and RP-32 reprogrammed MSC into the hindlimb musculature of immunodeficient mice to examine their capacity to support GSC1 in vivo growth and tumorigenicity. Generated tumors demonstrated higher tumor volume as compared with tumors generated by GSC1 grown in regular medium (Fig. 2E, 2F). However, only tumors generated by RP MSC revealed histological phenotypes similar to the phenotype observed in tumors generated by GSC1 coinjected with GSC-MSC, which also recapitulate the original patient-derived tumor phenotype (Fig. 2G). These tumors are characterized by a high degree of differentiation as indicated by the presence of tubular structures with fibroblast-like cells lining the spaces among the microscopic substructures of the tumor, with no observable necrosis within the tumor tissue.

In Vitro Organotypic Culture Model

To examine the role of GSC-MSC in supporting the growth of GSC1 cells, we established an in vitro organotypic culture model in which GSC1 and GSC-MSC are grown in a 3-dimensional (3D) culture. GSC1 by themselves did not sustain 3D culture growth beyond days 4–5. However, in the presence of GSC-MSC or RP MSC, the formation of organoid-like structures was observed, wherein the epithelial cancer cells were observed to line the margins (Fig. 3A). In order to delineate the composition of the 3D organoid-like structures, we transduced GSC1 with green fluorescent protein (GFP) and GSC-MSC with red fluorescent protein (RFP-tdTomato) expressing lentiviral vectors. Naïve T-MSC, and RP MSC RP-31 and RP-32 were also transduced with the tdTomato expressing vector. For generating organotypic culture, GFP-expressing GSC1 cells were grown together with tdTomato—expressing GSC-MSC. As shown in Figure 3B, during the first stages of organoid formation, GSC-MSC (in red) form spheroids. As early as 7 days, homing of GSC1 (in green) to these spheroids was observed. At later stages, GSC1 cells generated an epithelial structure that surround the MSC-derived spheroids (Fig. 3C). Organoids comprising GSC1 and GSC-MSC demonstrated high take rates when injected into the hindlimb musculature of immunodeficient mice by readily generating significantly larger tumors (~2.27 cm^3 at 4 weeks) in comparison with GSC1-derived spheroids (~0.3 cm^3 at 4 weeks; Fig. 3D). Interestingly, lung carcinoma-derived stromal cells (LC-MSC), which could not support the growth of GSC1 in vitro in a 2D culture or in vivo [38], also formed spheroids. However, GSC1 did not home in on them as efficiently as on GSC-MSC-derived spheroids (Fig. 3B). On the other hand, GSC1-mediated reprogrammed RP-31 and RP-32 MSC recapitulated the GSC1 organotypic 3D growth in the presence of GSC-MSC in contrast to T-MSC (Fig. 3E). These results further emphasize the tumor specific interaction between cancer cells and stromal cells and point to GSC1-mediated reprogrammed RP-31 and RP-32 MSC as GSC-MSC analogs in supporting GSC1 growth in vitro and in vivo.

Transcriptomic Profiling of GSC1-Mediated RP Cells

To decipher the mechanisms responsible for generating a tumor specific reactive stroma, we used the GSC1-RP T-MSC as a model to identify the alterations that GSC-MSC undergo within the tumor niche. For this purpose, gene expression profiles and transcriptome changes were compared between T-MSC, RP-31 and RP-32 MSC and GSC-MSC using RNA-Seq analyses. Changes detected in gene expression between T-MSC and their GSC-RP MSC counterparts were validated using Real-Time Quantitative Reverse Transcription polymerase chain reaction (qRT-PCR) and then examined in GSC-MSC. Since GSC-MSC and T-MSC are cells of different lineage backgrounds, we referred only to differentially expressed genes (DEGs) between T-MSC and RP-31 and RP-32 MSCs and validated their expression in GSC-MSC. DEGs were identified based on fold change (>2) and corresponding statistically significant *p*-values (<.05). GSC1 were used as a "readout" to examine the effect of changes in GSC-MSC on this tumor growth via cancer cell–stroma interaction. Principal component analysis was performed to assess the relative hierarchical contribution of

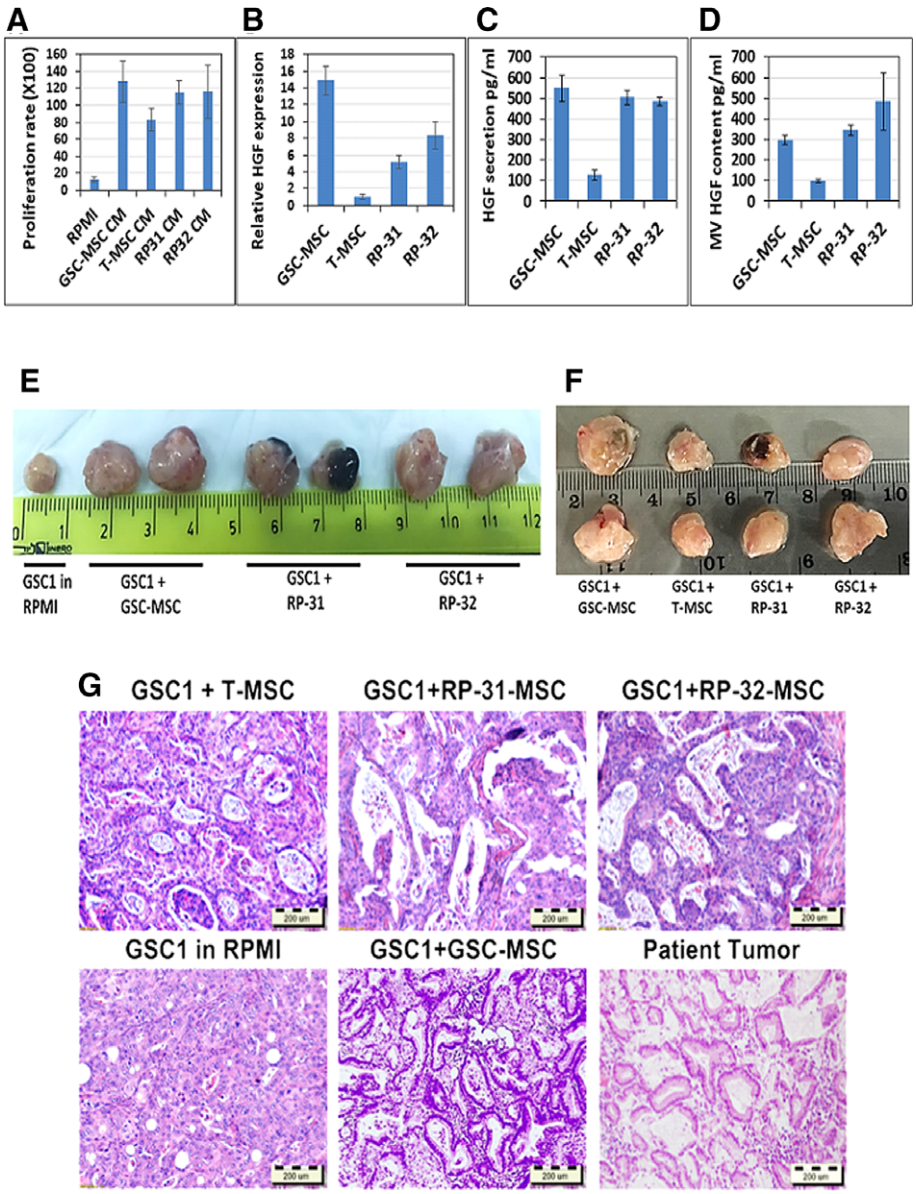

Figure 2. Reprogramming-mediated alteration of mesenchymal stem cell (MSC) supports gastric cancer cell (GSC1) growth. **(A):** The proliferation capacity of GSC1 cells grown in vitro in RPMI or in medium conditioned by GSC-MSC, T-MSC, reprogrammed (RP)-31 and RP-32 MSC as indicated. **(B):** RNA samples extracted from GSC-MSC, T-MSC, RP-31, and RP-32 MSC were subjected to qRT-PCR to examine the level of hepatic growth factor (HGF) gene expression. Expression levels were compared with T-MSC HGF expression level. Analyses were performed in triplicates using HPRT1 as an internal control. Bars and error bars represent means and SEM calculated for all samples in each group over two independent experiments. **(C):** The level of secreted HGF in GSC-MSC, T-MSC, RP-31, and RP-32 MSC was examined using enzyme-linked immunosorbent assay (ELISA). **(D):** The level of HGF captured in microvesicles (MV) derived from GSC-MSC, T-MSC, RP-31, and RP-32 MSC was examined using ELISA. **(E, F):** Tumorigenic capacity of GSC1 cancer cells was examined in vivo following injection of GSC1 cancer cells without or with GSC-MSC, T-MSC, RP-31, and RP-32 MSC, as indicated. Tumors were harvested at day 60 from injection. **(G):** The histological phenotype of the tumors presented in (E) was examined and compared with the original patient tumor histological phenotype. The blood observed in the tumor of the RP-31 group was identified as a hemorrhagic cyst, and histological examination did not reveal necrosis. Scale bars = 200 μm.

differences in gene expression among the samples (Supporting Information Fig. S1A). Distinct clustering of GSC-MSC, T-MSC, RP-31, and RP-32 samples was observed. A clustering relationship is evident between RP-31 and RP-32 samples (although originated from different mice) and T-MSC samples. Hierarchical cluster analysis of each sample in triplicate confirmed these findings (Supporting Information Fig. S1B). Expression levels for 29,997 genes in all four populations were obtained. The data was analyzed to identify genes that are most consistent with two patterns of interest—higher and lower expression levels in the RP populations (RP-31, RP-32, and GSC-MSC) compared with the T-MSC population. These two types of changes were termed reprogramming overexpression and reprogramming underexpression, respectively. We defined and calculated a single reprogramming factor for every gene (RepF[g]), as described in the "Materials and Methods" section. The resulting distribution of RepF(g) is provided in Supporting Information Figure S1C. Genes with RepF(g) significantly greater than

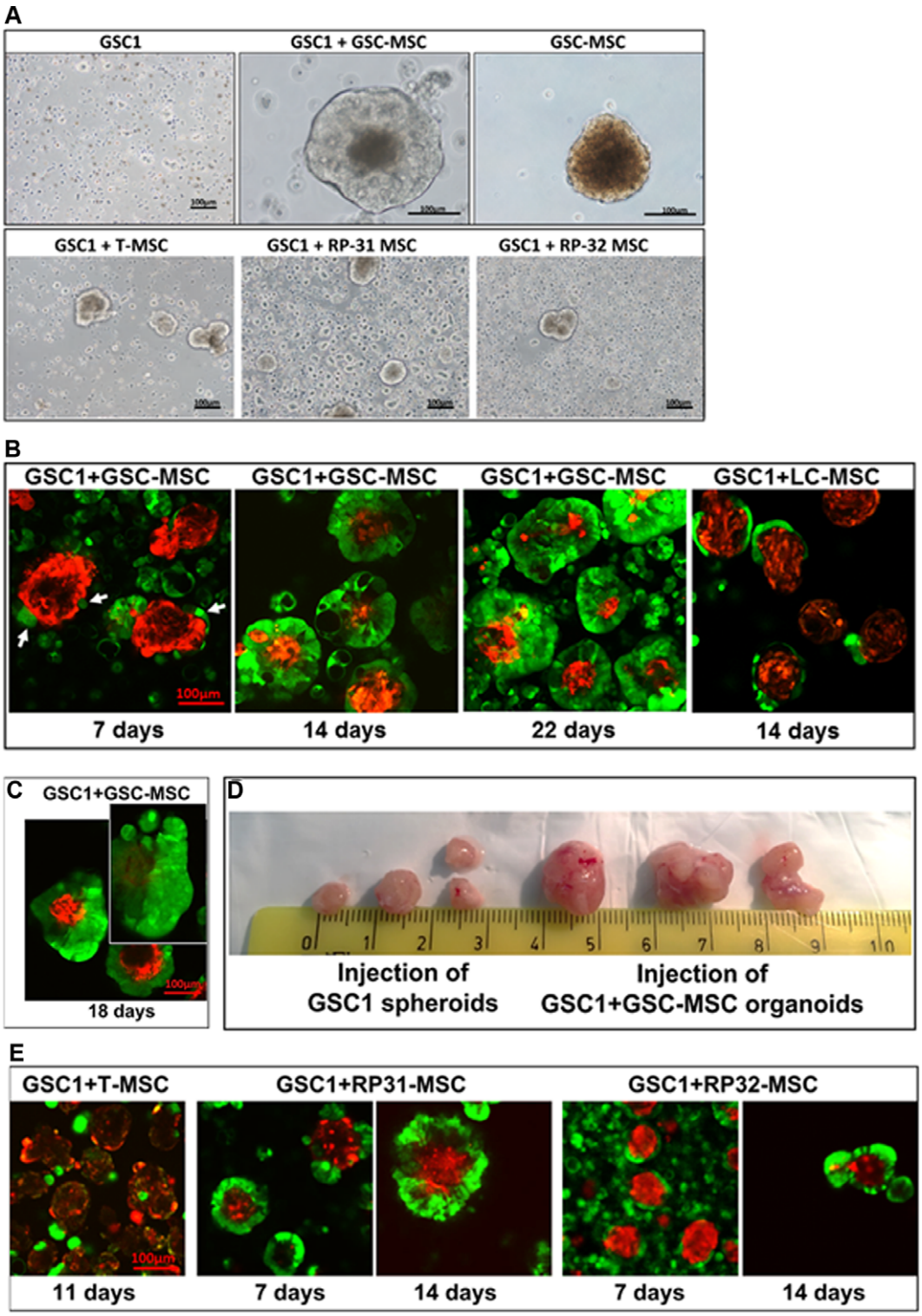

Figure 3. In vitro three-dimensional (3D) organotypic growth capacity of gastric cancer cell (GSC1) cancer cells. **(A):** GSC1 cells were grown in a 3D culture with GSC-mesenchymal stem cell (MSC), T-MSC, and RP-31 and RP-32 MSC. For comparison, GSC1 or GSC-MSC were grown in suspension as indicated. Scale bars = 100 µm. **(B):** Organoid formation in 3D growth. eGFP-expressing GSC1 (green) were grown together with tdTomato-expressing GSC-MSC (red) in suspension. First, GSC-MSC cells form spheroids and then GSC1 home on them to generate epithelial structures. Organoids were monitored at 7, 14, and 22 days as indicated. Organoid formation of GSC1 in the presence of lung carcinoma-derived MSC (LC-MSC) was monitored at day 14. Scale bar = 100 µm for all images. Using LSM 510 inverted microscope. **(C):** Generation of epithelial-like structures by GSC1 following homing on GSC-MSC derived spheroid in a 3D organotypic growth scale bar = 100 µm. **(D):** Tumors generated following injection of 5 days old GSC1-derived spheroids in comparison with 10 days old organoids comprised of GSC1 and GSC-MSC. Tumors were harvested at day 30 from injection. **(E):** Organoid formation in 3D growth of GSC1 together with naïve T-MSC and RP-31 and RP-32 as indicated. Scale bar = 100 µm for all images.

10 have higher expression in the RP populations compared with T-MSC expression (designated as 10), and those with values significantly smaller than 10 have relatively lower expression levels. Supporting Information Table S1 depicts the 200 genes with the highest reprogramming over expression and under expression values, respectively. This table also presents examples of the measured absolute expression levels for several genes from each of the categories—reprogramming overexpressed and reprogramming underexpressed. Furthermore, we validated these finding by qRT-PCR for several of these genes in comparison with their secretion levels measured by Human Cytokine Antibody Array as demonstrated in Supporting Information Figure S2. Of note, HGF which has been demonstrated to play a key role in GSC1 growth and proliferation in vitro and in vivo presents a high RepF score of 12.36. FGF7 which demonstrates an expression pattern similar to that of HGF following reprogramming, also has a high RepF score of 13.91. These genes are ranked 70 and 5 out of 29,996 genes, respectively. Notably, the mechanism of action for FGF7 did not involve support of GSC1 proliferation (data not shown). Another gene which presents a high RepF score of 14.0 is the ABCC3 multidrug-resistance transporter (ranked number 2).

Reciprocal Reprogramming Between GSC-MSC and GSC1 Cancer Cells Leads to Increased Expression of R-Spondin in GSC-MSC and Increased Expression of Lgr5 in GSC1 Cancer Cells

The RNA-Seq analyses of recruited "naïve" T-MSC and RP MSC RP-31 and RP-32 showed elevated expression levels of the genes RSPO1 and RSPO2 following reprogramming by GSC1 cancer cells, and this finding was validated by qRT-PCR (Fig. 4A). RSPO1 and RSPO2 genes encode for the R-spondin proteins, secreted agonists of the canonical Wnt/β-catenin signaling pathway [42]. Although R-spondins are unable to initiate Wnt signaling, they are necessary and sufficient for Wnt signal potentiation and enhancement following binding to the Lgr5 receptor [42]. Although RSPO3 and RSPO4 expression levels were also elevated following reprogramming as compared with T-MSC, GSC-MSC exhibited low expression levels of these genes (Fig. 4A). None of these cells expresses the LGR5 gene as was observed also in the RNA-Seq analysis and in the validation studies (Fig. 4A). To investigate the role of GSC-MSC secreted R-spondin in the tumor, we used GSC1 for readout of the changes related to activation of the R-spondin/Lgr5 signaling pathway. To this end, we took advantage of the conducted RNA-Seq analyses on GSC1 cancer cells grown in RPMI and in GSC-MSC CM (data not shown) to detect changes in the expression profiles. Interestingly, GSC1 express no or negligible levels of RSPO1-4. However, elevated expression levels of Lgr5, the receptor which binds R-spondin, were observed when GSC1 were grown in GSC-MSC CM (Fig. 4A). Lgr5 homologs, Lgr4 and Lgr6 which also bind R-spondin are expressed at a higher level in GSC1 (330, 1,900, and 3,348 reads, respectively). However, only Lgr5 expression levels were elevated when GSC1 grew in GSC-MSC CM (Fig. 4B). Elevated Lgr5 expression was also observed at the protein level in GSC1 grown in CM in a 2D culture as indicated by Western blot analysis (Fig. 4C). In a 3D culture, organoids comprising GSC-MSC and GSC1 demonstrate even higher (~sixfold) Lgr5 protein levels as compared with GSC1 spheroids grown in GSC-MSC CM. This contrasts with GSC-MSC grown without or with GSC1 CM, which express significantly lower levels of Lgr5 protein (as was also observed in RNA-Seq analyses, data not shown; Fig. 4B). These results point to a GSC-MSC-mediated paracrine R-spondin/Lgr5 signaling pathway in GSC1. Immunofluorescence analysis using anti-Lgr5 antibody indicated localization of Lgr5 protein to the cytoplasm, specifically around the nucleus, in all GSC1 grown in a 2D culture with or without GSC-MSC CM (Fig. 4D). A similar pattern of Lgr5 protein was observed in GSC1 grown together with GSC-MSC as organoids in 3D culture (Fig. 4E). Expression of Lgr5 was also observed in GSC-MSC when grown as spheroids in 3D culture (Fig. 4E). Since Lgr5 was previously associated with *stemness* both in adult stem cells and in CSC of the gastrointestinal tract in mice and in human [43–45], these results suggest that GSC1 might express their CSC potential in the presence of GSC-MSC.

Expression of Gastric Tumor CSC Specific Markers Lgr5 and CD133 In Vivo

Accumulating evidence suggests that CSC in the gastrointestinal tract express EpCAM, CD44, CD133 in addition to Lgr5 [46–49]. In agreement, FACS analyses of GSC1 cancer cells indicated expression of EpCAM, CD44 and CD133 in 100%, 97.8%, and 37.3%, respectively, when grown both in RPMI and in GSC-MSC CM (Supporting Information Fig. S3). On the other hand, qRT-PCR analysis to assess the expression levels of Oct4, Nanog, Sox2, and lin 28 *stemness* markers, indicated no or extremely low levels of expression of these genes in GSC1 cancer cells (data not shown). These results were confirmed by the RNA-Seq analyses, and are in agreement with a previous observation [41]. To examine whether GSC1 cancer cells express Lgr5 and CD133 in vivo, serial paraffin sections of tumors generated following intramuscular injection of GSC1 with and without GSC-MSC were examined by IHC using antihuman Lgr5 and CD133 antibodies. CD133, also known as prominin-1, is a transmembrane glycoprotein considered as a biomarker for CSC that have a critical role in recurrence of various malignancies including gastrointestinal tumors [50]. In tumors generated by GSC1 together with GSC-MSC, the results of these analyses exhibit clusters of Lgr5 and CD133 positively stained large tumor cells with large nuclei and a low cytoplasm/nucleus ratio. The negatively stained tumor cells contain smaller nuclei and a high cytoplasm/nucleus ratio, and they are organized in well-differentiated phenotypic structures (Fig. 4F). In tumors generated only by GSC1, the cancer cells were slightly and homogeneously stained for anti-Lgr5 antibody but were negatively stained for anti-CD133 antibody (Fig. 4F). Lgr5 and CD133 positively stained cells were also identified in paraffin sections of the original patient tumor (Fig. 4F). The negatively stained cells in these tumors were also organized into well differentiated structures. These results suggest that GSC-MSC might confer *stemness* properties and support gastric CSC in tumors generated in the presence of GSC-MSC.

GSC-MSC Mediated Activation of Wnt/β-Catenin Pathway and β-Catenin Localization In Vitro

Accumulating evidence supports the observation that RSPO binding to Lgr5 stimulates the canonical Wnt/β-catenin pathway through enhancing phosphorylation of the low-density lipoprotein receptor-related protein 5/6 coreceptors (LRP5/6) [51]. RSPO can also interact with the cell surface E3-ligases

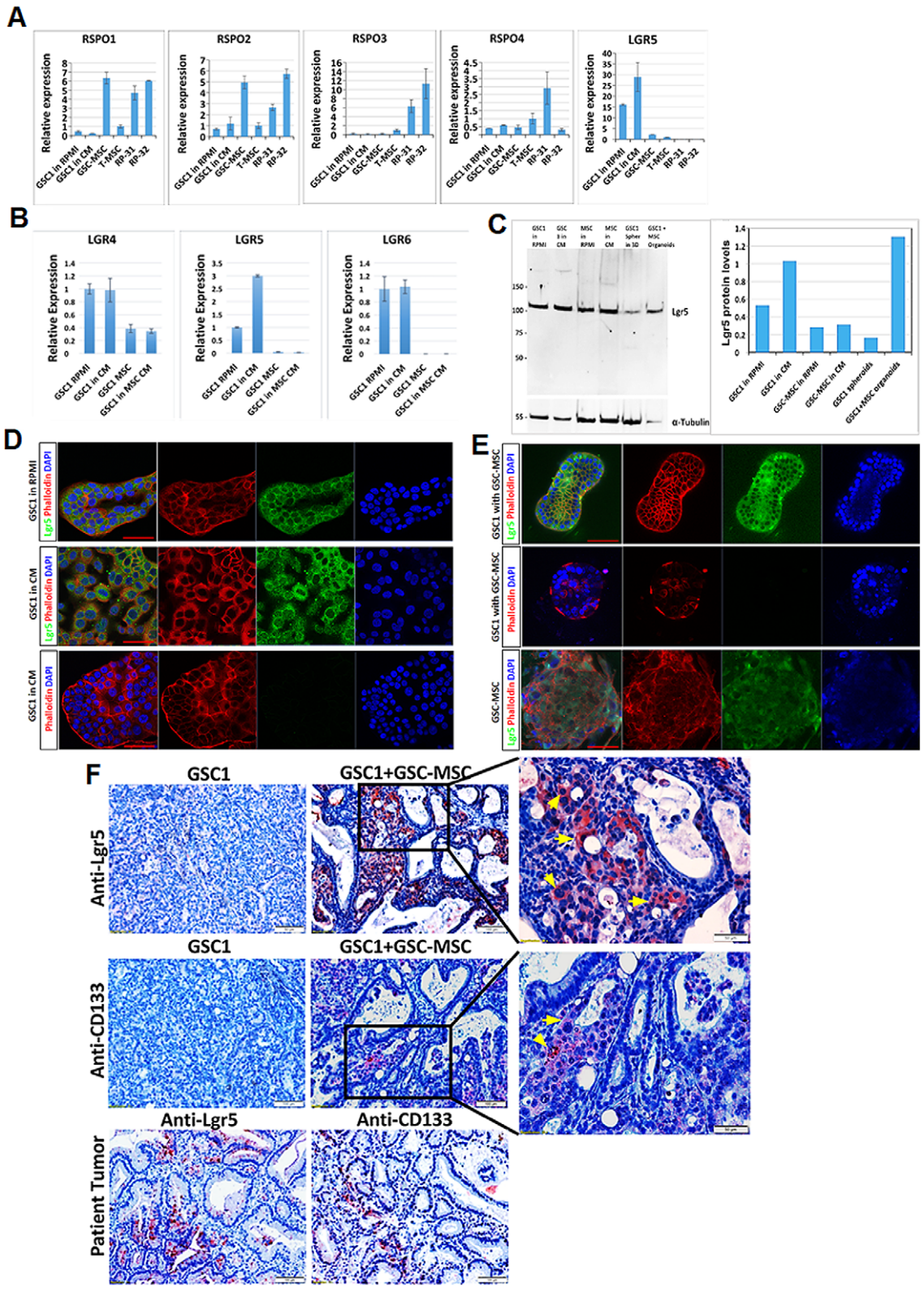

Figure 4. Expression of R-spondin (RSPO) in gastric cancer cell-derived mesenchymal stem cell (GSC-MSC) and Lgr5 in GSC1 cancer cells. **(A):** RNA samples extracted from GSC1 grown in RPMI or in GSC-MSC CM, GSC-MSC, recruited "naïve" T-MSC and RP-31 and RP-32 MSC, were subjected to qRT-PCR with specific primers for RSPO1-4 and Lgr5 genes. Expression of the indicated genes in the various RNA samples are demonstrated relative to naïve T-MSC (T-MSC expression level = 1). Analyses were performed in triplicate using HPRT1 as an internal control. Bars and error bars represent means and SEM calculated for all samples in each group over two independent experiments. **(B):** The influence of GSC1 and GSC-MSC interaction on Lgr4, Lgr5, and Lgr6 gene expression was monitored by using qRT-PCR analysis in GSC1 grown in RPMI and in GSC-MSC CM and on GSC-MSC grown in RPMI and in GSC1 CM. Expression of the indicated genes

(Figure legend continues on next page.)

ZNRF3 and RNF43, which regulate the cell surface expression of the Wnt receptor complex [52]. Binding of RSPO to Lgr5 and to ZNRF3/RNF43 induces their internalization and prevents the inhibitory ubiquitylation of LRPs [53]. At the intestinal crypt bottom, Paneth cells and stromal cells supply Wnt ligands and the Wnt coagonist R-spondin to sustain the self-renewal of Lgr5+ crypt stem cells through stimulating the Wnt/β-catenin signaling pathway [54]. Activation of the canonical Wnt signaling pathway leads to the disruption of the β-catenin degradation complex, accumulation of β-catenin in the cytoplasm and translocation of β-catenin to the nucleus, where it activates the transcription of canonical Wnt target genes [42, 55–57]. Therefore, we sought to determine whether *stemness* of GSC1 epithelial cancer cells might be governed by the MSC component of the TME. First, we observed differential expression of Lgr5 when GSC1 cells were grown in GSC-MSC CM as compared with RPMI (Fig. 5A). This contrasts with no difference in expression of β-catenin and its target genes Axin2 and RNF43. We sought to examine whether GSC-MSC-mediated induction of Lgr5 in GSC1 coactivates the Wnt/β-catenin signaling pathway as a possible mechanism to support gastric CSC. For this purpose, anti-β-catenin antibody was used for immunofluorescence analysis of the expression and localization of β-catenin in GSC1 grown in vitro in a 2D culture with or without GSC-MSC CM. In both culture conditions, distinct expression of β-catenin can be observed in the cell membrane. Screening examination of the entire culture plate did not indicate β-catenin localization to the cell nucleus under these growth conditions (Fig. 5B). Similar analysis performed in organoids comprising GSC1 grown together with GSC-MSC cells in a 3D culture, revealed low numbers of GSC1 cells which expressed β-catenin in the cell nucleus, suggesting that despite Lgr5 expression across all GSC1 cells, only few activate the Wnt/β-catenin signaling pathway (Fig. 5C and Supporting Information Fig. S4). Next, the activation of Wnt/β-catenin signaling pathway in GSC1 cells was assessed using a β-catenin/TCF transcription-based reporter construct. GSC1 were transduced with the 7TGC lentiviral vector which carries an SV40-mCherry selection cassette downstream of the 7xTcf-eGFP reporter cassette [58]. Cells infected with the 7TGC virus display red fluorescence, while activation of the Wnt/β-catenin signaling pathway induces also expression of eGFP in the cells. Infected cells were selected by FACS according to mCherry expression, and grown in either a 2D culture in GSC-MSC CM, or in a 3D culture as organoids with nonstained, noninfected GSC-MSC. Sparse colonies of GSC1 expressing both mCherry and eGFP were observed in 2D culture, indicating activation of the Wnt/β-catenin signaling pathway in these cells (Fig. 5D). On the other hand, organoids generated by 7TGC-expressing GSC1 and unmodified MSC-GSC1 demonstrate the existence of cells with both mCherry and eGFP expression, pointing to Wnt/β-catenin signaling pathway induced translocation of β-catenin to the nucleus (Fig. 6A). These results suggest that GSC-MSC confer and sustain *stemness* in GSC1 cells present in such organoids. Interestingly, GSC1 cells that expressed both mCherry and GFP did spontaneously form spheroids in a 2D culture following collection by FACS (~1.2% of the cells), however, spheroid formation was restricted to GSC-MSC CM growth condition (Fig. 6B). Nevertheless, organoids formed by these mCherry and GFP expressing GSC1 cells together with nonstained, noninfected GSC-MSC, indicated that these green GSC1 cells were organized in a columnar epithelial like formation surrounding the GSC-MSC derived spheroid (Fig. 6B).

GSC-MSC-Induced β-Catenin Nuclear Localization in Gastric Tumors In Vivo

To examine whether GSC-MSC confer *stemness* properties and maintain CSC in gastric tumors in vivo, serial paraffin sections of tumors generated by GSC1 injected without or with GSC-MSC were analyzed for β-catenin expression using IHC (referring to the tumor sections described in Fig. 4F). Tumors generated from only GSC1 exhibit a homogeneous histological phenotype in which high intensity staining for anti-β-catenin was identified in the cells localized in the tumor margins. β-Catenin positive staining progressively diminished toward the center of the tumor. Localization of β-catenin to the cell membrane suggests the involvement of β-catenin in adhesion of these cells. Surprisingly, tumors generated by injection of GSC1 together with GSC-MSC revealed a complete change in the β-catenin localization pattern in the tumor. In this case, β-catenin positively stained cells appeared in clusters in which β-catenin is localized to the cell nucleus (Fig. 6C). Importantly, the clusters of β-catenin positive cells overlap the clusters of Lgr5 positive cells shown in Figure 4F. However, not all the Lgr5 positive cells express β-catenin (Fig. 6D). Taken together, these results suggest that GSC-MSC induce *stemness* properties in Lgr5-positive GSC1 through secretion of R-spondin and activation of the Wnt/β-catenin signaling pathway which eventually leads to translocation

(Figure legend continued from previous page.)
in the various RNA samples are demonstrated relative to GSC1 grown in RPMI (expression level = 1). Analyses were performed in triplicates using HPRT1 as an internal control. Bars and error bars represent means and SEM calculated for all samples in each group over two independent experiments. **(C):** Lgr5 protein level in GSC1 and GSC-MSC grown in vitro. Plasma membrane proteins were extracted from GSC1 cancer cells grown in vitro in two-dimensional (2D) and 3D culture in various conditions as indicated. Lgr5 protein level was assessed by Western blot analysis with antihuman Lgr5 antibody (left panel). Lgr5 protein level was measured using the Totallab quantification program as presented in the right panel. Anti-α-tubulin antibody was used for protein sample quantification. **(D):** Expression of Lgr5 in GSC1 grown in a 2D culture in RPMI (upper panel) or in GSC-MSC CM (middle panel) were subjected to immunofluorescence analysis using anti-Lgr5 antibodies (green). Phalloidin was used for staining F-actin in the cell membrane (red) and DAPI was used for nuclei staining (blue). Lower panel represents no primary antibody control. Bar = 50 μm for all images, using the LSM700 microscope. **(E):** Expression of Lgr5 in in vitro grown organoids. GSC1 and GSC-MSC grown in a 3D culture were subjected to immunofluorescence analysis (upper panel) using anti-Lgr5 antibodies (green). Phalloidin was used for staining F-actin in the cell membrane (red) and DAPI was used for nuclei staining (blue). Middle panel represents no primary antibody control. Lower panels demonstrate staining of a GSC-MSC derived spheroid. Bar = 50 μm for all images, using the LSM700 microscope. **(F):** Expression of gastric cancer stem cell markers LGR5 and CD133 in vivo. Paraffin sections of tumors generated by GSC1 injected with or without GSC-MSC into the hindlimb musculature of SCID/beige mice were stained with anti-LGR5 and anti-CD133, as indicated. Lgr5 and CD133 positive cells were also detected in paraffin sections of the original patient tumor. The depicted areas in the upper and middle panels are enlarged in the right panels. Arrows indicate clusters of cells positively stained with anti-LGR5 and CD133. Bars = 100 μm for the left panels and 50 μm for the enlarged panels.

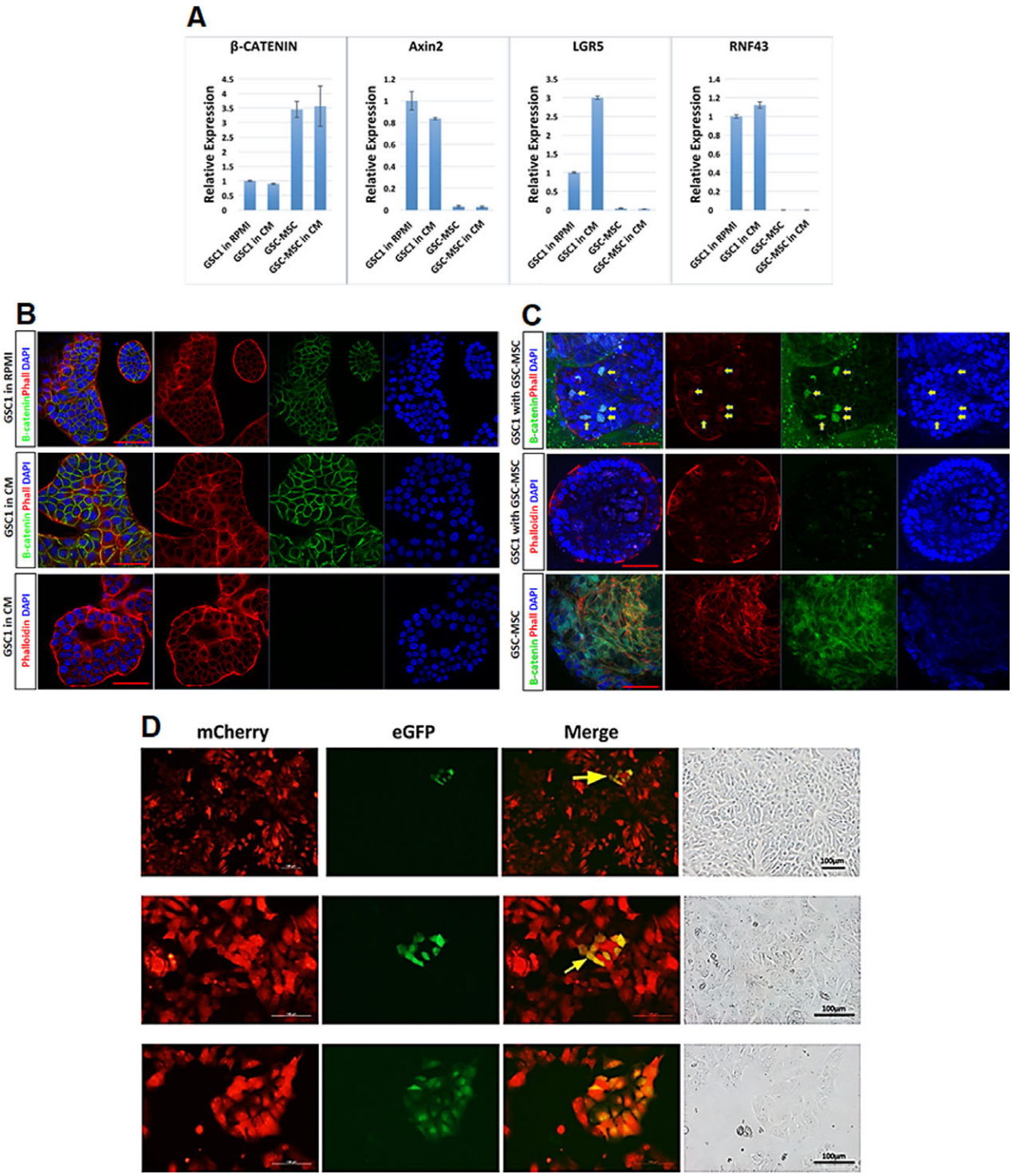

Figure 5. Gastric cancer cell-derived mesenchymal stem cell (GSC-MSC) mediated activation of Wnt/β-catenin pathway and β-catenin localization in vitro. **(A):** The effect of GSC1 and GSC-MSC interaction on β-catenin and Wnt targeted genes Axin 2, Lgr5 and RNF43 was monitored using qRT-PCR analyses with specific primers. RNA was extracted from GSC1 cancer cells grown in RPMI and in GSC-MSC conditioned medium (CM) and from GSC-MSC grown in RPMI and in GSC1 CM. Expression of the indicated genes in the various RNA samples are demonstrated relative to GSC1 grown in RPMI (expression level = 1). Analyses were performed in triplicates using HPRT1 as an internal control. Bars and error bars represent mean and SEM calculated for all samples in each group over two independent experiments. **(B):** Expression of β-catenin in GSC1 grown in a two-dimensional culture in RPMI (upper panel) or in GSC-MSC CM (middle panel) were subjected to immunofluorescence analysis using anti-β-catenin antibody (green). Phalloidin was used for staining F-actin in the cell membrane (red) and DAPI was used for nuclei staining (blue). Lower panel represents no primary antibody control. Bar = 50 μm for all images, using the LSM700 microscope. **(C):** Expression of β-catenin in in vitro grown organoids. GSC1 and GSC-MSC grown in a 3D culture were subjected to immunofluorescence analysis (upper panel) using anti-β-catenin antibody (green). Phalloidin was used for staining F-actin in

(Figure legend continues on next page.)

of β-catenin into the cancer cells nuclei for transcriptional activation of downstream targets.

Discussion

In the process of tumor formation, the specification and proper arrangements of heterogeneous cell types occur through the coordinated regulation of gene expression and interactions between cancer cells and neighboring stromal cells which are recruited into the tumor niche to support the tumor cells. An important goal is to identify the signaling pathways that coordinate dynamic changes in gene expression which mutually influence properties of heterogeneous cancer cells including CSC and their supporting stromal cells within the TME [18, 19]. The signaling pathways responsible for these functions are induced by extracellular ligands and their receptors, and modify cancer cell properties, such as *stemness*, survival, proliferation, adhesion and migration. In the current study, we demonstrate an extreme, but illustrative example in which the "seeds" of tumor cancer cells subvert the "soil" in a way that shapes the nature of the tumor MSC component to serve tumor progression. Increasing evidence indicates that CSC comprise a distinct self-renewing subpopulation with reduced replicative potency that can initiate tumors and mediate recurrence and metastasis. Most anticancer cell cycle active drugs kill the bulk of cancer cell populations and skip CSC as they divide rarely and can escape chemotherapy by drug expulsion [59]. The Wnt signaling pathway is a powerful regulator of cell proliferation and differentiation, which involves proteins that directly participate in both gene transcription and cell adhesion. The central player of this pathway is β-catenin, which can act as a transcription cofactor and a structural adaptor protein linking cadherins to the actin cytoskeleton to achieve cell–cell adhesion [60, 61]. Misguided interactions of β-catenin with adhesion molecules in the cell membrane, with a destruction complex in the cytoplasm or with a transcription complex in the nucleus can lead to tumor formation [60, 62]. Lgr5 is a Wnt target gene that marks adult stem cells with self-renewal activity in the intestinal crypt and CSC in gastrointestinal tumors [54]. The fact that Lgr5 acts as receptor for R-spondin, reinforces the linkage between Wnt signaling and activation of stem cells in normal developmental and in tumorigenic processes [56]. In the normal intestinal crypt, Lgr5 stem cells receive essential niche support from their own specialized progeny Paneth cells which provide them with Wnt signals to maintain their *stemness* properties [54]. Lgr5 is also associated with *stemness* properties in CSC in gastrointestinal tumors in mice and in human [44, 45]. Recently, we reported on the specific contribution of HGF-secreting tumor-derived MSC to in vivo tumorigenic capacity in gastric carcinoma. Moreover, we described the "basic skills" of the GSCs to recruit specific competent HGF-secreting "naïve" MSC from the adjacent tissue in the process of tumorigenesis and to educate/reprogram them in a tumor type specific manner to support tumor progression [38]. In the current study, we took advantage of this gastric tumor, in which the GSC1 cells critically depend on their GSC-MSC tumor counterpart, as a model to examine the interplay between these two components that leads to generation of tumor reactive stroma. A marked elevation of HGF expression and secretion levels was identified in primed RP-31 and RP-32 reprogrammed MSC as compared with GSC-MSC, pointing to the changes naïve T-MSC undergo to become qualified to support GSC1 proliferation capacity. Similar to what we describe here, it has been reported that HGF secreted by myofibroblasts in colon tumors exhibited an enhanced Wnt signaling pathway, activation of β-catenin-dependent transcription and subsequently enhancement of CSC clonogenicity [63].

Significantly increased expression of ABCC3, a multidrug-resistance family member, was also observed in primed RP-31 and RP-31 and RP-32 reprogrammed MSC, which follows the same line of elevated expression levels for the ABCB1 gene in GSC-MSC [38]. The ABC transporters are responsible for decreased drug accumulation in drug-resistant cells and often mediate cancer cell survival despite anticancer therapy reagents [64]. The extremely high expression level of the ABCB1 gene in GSC-MSC stromal cells enables them to avoid eradication by cytotoxic effects, thereby providing a continuous support for their cancer cell counterpart in the tumor. The patient, from whom the GSC1 cancer cells were derived, was treated with chemotherapeutic agents which are substrates for those transporters. This also reminds us that reprogramming affects a process wherein rare MSC have been recruited and evoke such an effect. Those which remain, have been selected to support tumor growth. In this regard, it will be important to investigate the detailed mechanism(s) underlying the reprogramming of MSC by GSC1 cancer cells, which leads to generation of a more powerfully tumor supportive niche.

Primed RP-31 and RP-32 reprogrammed MSC resemble GSC-MSC also in supporting in vitro 3D growth of GSC1, which do not form spheroids by themselves. GSC1 cells can home specifically to GSC-MSC or primed MSC-derived spheroid and generate epithelial structures in organotypic growth in contrast to T-MSC and LC-MSC. In addition, primed MSC exhibited GSC1 growth support in vivo by their capacity to recapitulate both the tumor volume and the phenotypic histological appearance observed in the case of GSC-MSC grown with GSC1 cells and the original tumor. It is important to note that T-MSC which were specifically recruited by GSC1 cancer cells from the adjacent tissue also support GSC1 in vivo growth but the histological phenotype of the generated tumors indicate that they are not fully equipped with tumor promoting capacity as observed for RP MSC. These results indicate that the paracrine effect of GSC-MSC is sufficient for a 2D growth of GSC1, however, cell–cell interaction with the tumor specific

(Figure legend continued from previous page.)
the cell membrane (red) and DAPI was used for nuclei staining (blue). Middle panel represents no primary antibody control. Lower panels demonstrate staining of GSC-MSC derived spheroid. Arrows indicate cell nuclei positively stained with anti-β-catenin antibody (upper panel). Bar = 50 μm for all images, using the LSM700 microscope. **(D):** Induction of β-catenin nuclear localization in GSC1 in vitro was assessed by using a β-catenin/TCF transcription-based reporter construct. GSC1 transduced with the 7TGC lentiviral vector display mCherry red fluorescence (left panels). Activation of the Wnt/β-catenin signaling pathway induces expression of eGFP in the cells (middle panels). Merged expression of mCherry and eGFP are presented in yellow. Bars = 100 μm for all images.

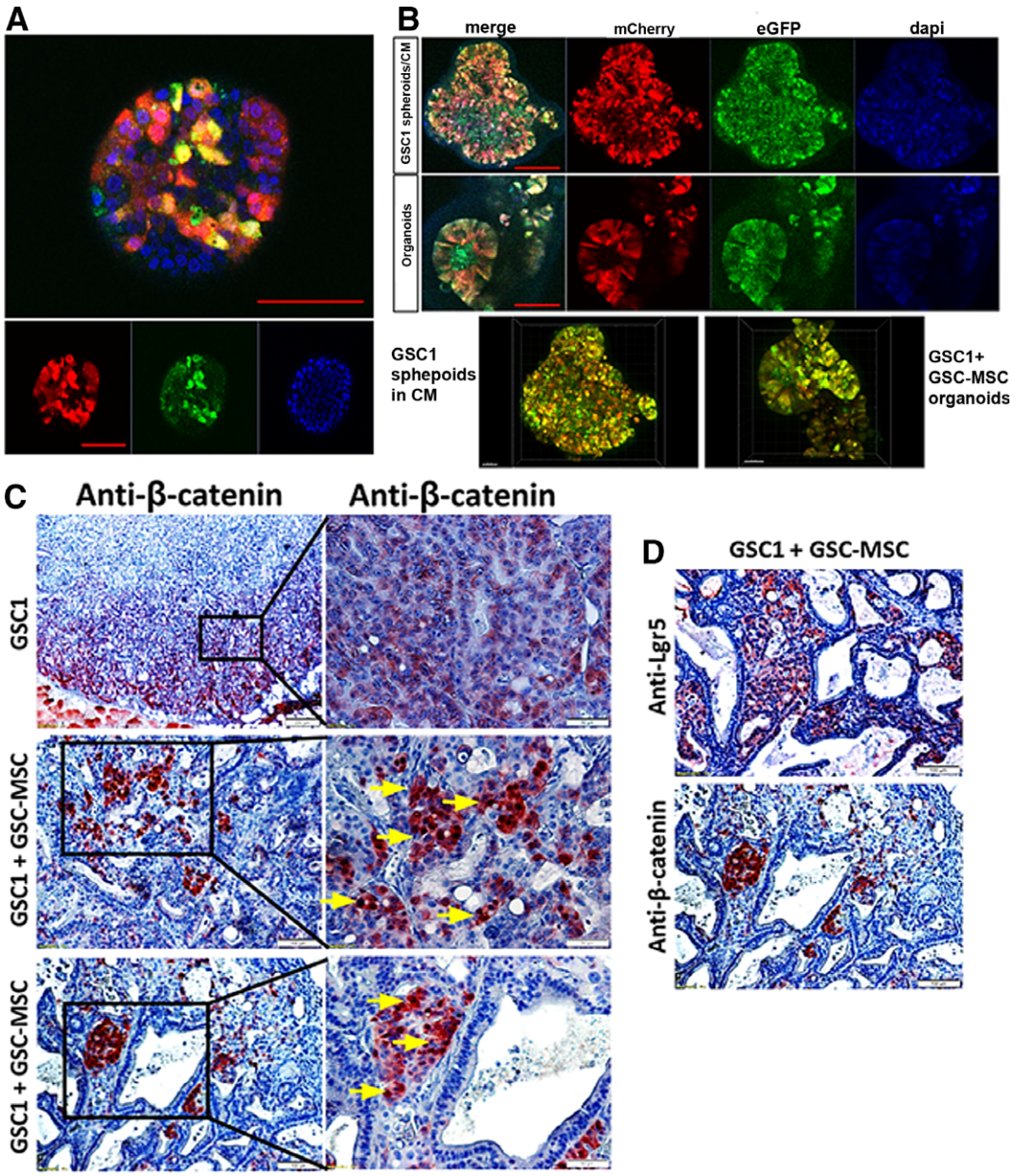

Figure 6. Gastric cancer cell-derived mesenchymal stem cell (GSC-MSC)-induced β-catenin nuclear localization in organoids and in gastric tumors in vivo. **(A):** Expression and localization of β-catenin in organoids comprised of GSC1 cancer cells and GSC-MSC. Transduced GSC1 used for this organotipic growth display constitutive mCherry red fluorescence and β-catenin/TCF transcription induction of eGFP. Bar = 50 μm, using the LSM880 microscope. **(B):** Transduced GSC1 cells which express both mCherry and eGFP form spheroids in a three-dimensional (3D) culture in CM (upper panel), and organoids together with nonstained nontransformed GSC-MSC (middle panel). Lower panel exhibit 3D images prepared using the Imaris software. Bar = 50 μm for all images, using the LSM880 microscope. **(C):** Expression and localization of β-catenin in gastric tumors in vivo. Paraffin sections of tumors generated by GSC1 injected with or without GSC-MSC into the hindlimb musculature of SCID/beige mice were stained with anti-β-catenin antibodies as indicated. Serial sections are referring to the paraffin sections described in Figure 4F. The depicted areas in the left panels are enlarged in the right panels. Arrows indicate clusters of cells positively stained with anti-β-catenin. Bars = 100 μm for the left panels and 50 μm for the enlarged right panels.

stromal cells GSC-MSC or their homolog primed RP-31 and RP-32 MSC are necessary for 3D growth and for in vivo tumor formation. Paracrine and juxtacrine mediated elevation of Lgr5 expression at both the transcription and the protein levels suggest GSC-MSC mediated *stemness* support in GSC1 cancer cells in vitro. However, GSC1 cells do not express the RSPO1 and two genes which encode for the Lgr5 receptor ligand R-spondin, as compared with GSC-MSC. The interplay between GSC1 cancer cells and GSC-MSC observed for the HGF/cMET signaling pathway [38], is augmented in the case of the R-spondin/Lgr5 axis, consistent with WNT/β-catenin signaling pathway involvement in maintaining CSC properties. Although Lgr5 expression is observed in all GSC1 cancer cells grown in vitro in a 2D culture in CM, and in 3D cultures together with GSC-MSC, only ~1.2% of this Lgr5+ GSC1 cell population exhibit the activation of WNT/β-catenin signaling pathway and translocation of β-catenin into the nucleus. Only these cells are capable of spheroid formation when grown by themselves in a 3D

culture, results which are consistent with CSC properties. Future studies will be needed to verify conclusively that these are CSC by using in vivo serial passages.

The RP MSC effect on GSC1 cancer cell *stemness* is most strikingly evident in vivo. In this case, injection of Lgr5+ GSC1 cells together with GSC-MSC results in clusters of large Lgr5+ cells that can both self-renew and differentiate into smaller nonstem Lgr5− cells. Thus, GSC-MSC confer *stemness* properties to Lgr5+ GSC1 cancer cells, as demonstrated by the appearance of β-catenin-positive clusters of cells, in which β-catenin expression is localized to the nucleus. The latter indicate the activation of the WNT/β-catenin signaling pathway. There is evident overlap of β-catenin positive clusters of cells with the Lgr5 positive cluster of cells. However, not all Lgr5+ cells express β-catenin. These results suggest that Lgr5 is necessary but not sufficient to maintain Wnt/β-catenin activated CSC in this gastric tumor. These observations suggest that potential Lgr5+ CSC exist in GSC1 derived tumors, however, their CSC potential requires the presence of the RP MSC component of the TME within the entire tumor milieu. In future studies it will be of particular interest to examine the involvement of the R-spondin/Lgr5 interaction and wnt/β-catenin signaling pathways in GSC1 and GSC-MSC reciprocal reprograming.

Conclusion

The results of the current study provide a basis for elucidating the signaling interactions between cancer cells and the stromal cells which are recruited into the tumor niche. The approach described herein succeeded in uncovering the subversion of gene expression and cytokine production by MSC recruited into the TME, and the prominent contribution of this process in sustaining the cancer stem cell underpinnings of tumor progression.

Acknowledgments

We thank Gal Akiri for helpful discussions. We thank Sara Selig and Ayala Ofir for critical reading of the manuscript, and Irena Reiter and Nisreen Hassan for excellent technical assistance. We thank Liat Linde, Ronit Modai-Hod, and Nili Avidan for excellent bioinformatics assistance. We also thank Maya Holdengreber Edith Suss-Toby and Melia Gurewitz for excellent bioimaging assistance. This research was supported by grants from the Daniel M. Soref Charitable Trust, the Skirball Foundation, and the ATS-Stem Cell Research Foundation.

Author Contributions

Y.S.: conception and design, collection and assembly of data, data analysis and interpretation, manuscript writing, final approval of manuscript; D.C.A.: data analysis and interpretation, final approval of manuscript; Z.Y.: data analysis and interpretation, final approval of manuscript; K.S.: conception and design, financial support, data analysis and interpretation, manuscript writing, final approval of manuscript; M.T.: conception and design, financial support, collection and assembly of data, data analysis and interpretation, manuscript writing, final approval of manuscript.

Disclosure of Potential Conflicts of Interest

The authors indicated no potential conflicts of interest.

References

1 Junttila MR, de Sauvage FJ. Influence of tumour micro-environment heterogeneity on therapeutic response. Nature 2013;501:346–354.

2 Bergfeld SA, DeClerck YA. Bone marrow-derived mesenchymal stem cells and the tumor microenvironment. Cancer Metastasis Rev 2010;29:249–261.

3 Kalluri R, Zeisberg M. Fibroblasts in cancer. Nat Rev Cancer 2006;6:392–401.

4 Sung SY, Hsieh CL, Wu D et al. Tumor microenvironment promotes cancer progression, metastasis, and therapeutic resistance. Curr Probl Cancer 2007;31:36–100.

5 Quante M, Tu SP, Tomita H et al. Bone marrow-derived myofibroblasts contribute to the mesenchymal stem cell niche and promote tumor growth. Cancer Cell 2011;19:257–272.

6 Karnoub AE, Dash AB, Vo AP et al. Mesenchymal stem cells within tumour stroma promote breast cancer metastasis. Nature 2007;449:557–563.

7 Hanahan D, Coussens LM. Accessories to the crime: Functions of cells recruited to the tumor microenvironment. Cancer Cell 2012;21:309–322.

8 Orimo A, Weinberg RA. Stromal fibroblasts in cancer: A novel tumor-promoting cell type. Cell Cycle 2006;5:1597–1601.

9 Nishimura K, Semba S, Aoyagi K et al. Mesenchymal stem cells provide an advantageous tumor microenvironment for the restoration of cancer stem cells. Pathobiology 2012;79:290–306.

10 Kansy BA, Dissmann PA, Hemeda H et al. The bidirectional tumor–Mesenchymal stromal cell interaction promotes the progression of head and neck cancer. Stem Cell Res Ther 2014;5:95.

11 Sun Z, Wang S, Zhao RC. The roles of mesenchymal stem cells in tumor inflammatory microenvironment. J Hematol Oncol 2014;7:14.

12 Pap E. The role of microvesicles in malignancies. Adv Exp Med Biol 2011;714:183–199.

13 D'Souza-Schorey C, Clancy JW. Tumor-derived microvesicles: Shedding light on novel microenvironment modulators and prospective cancer biomarkers. Genes Dev 2012;26:1287–1299.

14 Muralidharan-Chari V, Clancy JW, Sedgwick A et al. Microvesicles: Mediators of extracellular communication during cancer progression. J Cell Sci 2010;123:1603–1611.

15 Marusyk A, Polyak K. Tumor heterogeneity: Causes and consequences. Biochim Biophys Acta 2010;1805:105–117.

16 Polyak K, Haviv I, Campbell IG. Co-evolution of tumor cells and their microenvironment. Trends Genet 2009;25:30–38.

17 Shackleton M, Quintana E, Fearon ER et al. Heterogeneity in cancer: Cancer stem cells versus clonal evolution. Cell 2009;138:822–829.

18 Abelson S, Shamai Y, Berger L et al. Intratumoral heterogeneity in the self-renewal and tumorigenic differentiation of ovarian cancer. Stem Cells 2012;30:415–424.

19 Abelson S, Shamai Y, Berger L et al. Niche-dependent gene expression profile of intratumoral heterogeneous ovarian cancer stem cell populations. PLoS ONE 2013;8:e83651.

20 Gerlinger M, Rowan AJ, Horswell S et al. Intratumor heterogeneity and branched evolution revealed by multiregion sequencing. N Engl J Med 2012;366:883–892.

21 Yap TA, Gerlinger M, Futreal PA et al. Intratumor heterogeneity: Seeing the wood for the trees. Sci Transl Med 2012;4:127ps110.

22 Kreso A, O'Brien CA, van Galen P et al. Variable clonal repopulation dynamics influence chemotherapy response in colorectal cancer. Science 2013;339:543–548.

23 Gupta PB, Chaffer CL, Weinberg RA. Cancer stem cells: Mirage or reality? Nat Med 2009;15:1010–1012.

24 Hanahan D, Weinberg RA. Hallmarks of cancer: The next generation. Cell 2011;144: 646–674.

25 Scheel C, Weinberg RA. Cancer stem cells and epithelial–mesenchymal transition: Concepts and molecular links. Semin Cancer Biol 2012;22:396–403.

26 van der Horst G, Bos L, van der Pluijm G. Epithelial plasticity, cancer stem cells, and the tumor-supportive stroma in bladder carcinoma. Mol Cancer Res 2012;10:995–1009.

27 Ebben JD, Treisman DM, Zorniak M et al. The cancer stem cell paradigm: A new understanding of tumor development and treatment. Expert Opin Ther Targets 2010;14: 621–632.

28 Borovski T, De Sousa EMF, Vermeulen L et al. Cancer stem cell niche: The place to be. Cancer Res 2011;71:634–639.

29 Clevers H. The cancer stem cell: Premises, promises and challenges. Nat Med 2011;17:313–319.

30 Marin JJ, Al-Abdulla R, Lozano E et al. Mechanisms of resistance to chemotherapy in gastric cancer. Anticancer Agents Med Chem 2015;16:318–334.

31 Meads MB, Gatenby RA, Dalton WS. Environment-mediated drug resistance: A major contributor to minimal residual disease. Nat Rev Cancer 2009;9:665–674.

32 Tiago M, de Oliveira EM, Brohem CA et al. Fibroblasts protect melanoma cells from the cytotoxic effects of doxorubicin. Tissue Eng Part A 2014;20:2412–2421.

33 Straussman R, Morikawa T, Shee K et al. Tumour micro-environment elicits innate resistance to RAF inhibitors through HGF secretion. Nature 2012;487:500–504.

34 Wang X, Zou F, Deng H et al. Characterization of sphereforming cells with stemlike properties from the gastric cancer cell lines MKN45 and SGC7901. Mol Med Rep 2014;10: 2937–2941.

35 Tian T, Zhang Y, Wang S et al. Sox2 enhances the tumorigenicity and chemoresistance of cancer stem-like cells derived from gastric cancer. J Biomed Res 2012;26:336–345.

36 Chen XL, Chen XZ, Wang YG et al. Clinical significance of putative markers of cancer stem cells in gastric cancer: A retrospective cohort study. Oncotarget 2016;7:62049–62069.

37 Rassouli FB, Matin MM, Saeinasab M. Cancer stem cells in human digestive tract malignancies. Tumour Biol 2016;37:7–21.

38 Berger L, Shamai Y, Skorecki K et al. Tumor specific recruitment and reprogramming of mesenchymal stem cells in tumorigenesis. Stem Cells 2015;34:1011–1026.

39 Tzukerman MSY, Cohn Alperovich D, Yakhini Z et al. Shaping the soil for the seeds: Reciprocal reprogramming of cancer cells and associated mesenchymal stem cells in gastric cancer. Cancer Microenviron 2018; Suppl 1:1-91. https://doi.org/10.1007/s12307-018-0212-6.

40 Dominici M, Le Blanc K, Mueller I et al. Minimal criteria for defining multipotent mesenchymal stromal cells. The International Society for Cellular Therapy position statement. Cytotherapy 2006;8:315–317.

41 Schoenhals M, Kassambara A, De Vos J et al. Embryonic stem cell markers expression in cancers. Biochem Biophys Res Commun 2009;383:157–162.

42 de Lau W, Peng WC, Gros P et al. The R-spondin/Lgr5/Rnf43 module: Regulator of Wnt signal strength. Genes Dev 2014;28: 305–316.

43 Barker N, Ridgway RA, van Es JH et al. Crypt stem cells as the cells-of-origin of intestinal cancer. Nature 2009;457:608–611.

44 Schepers AG, Snippert HJ, Stange DE et al. Lineage tracing reveals Lgr5(+) stem cell activity in mouse intestinal adenomas. Science 2012;337:730–735.

45 Wang B, Chen QT, Cao Y et al. LGR5 is a gastric cancer stem cell marker associated with stemness and the EMT signature genes NANOG, NANOGP8, PRRX1, TWIST1, and BMI1. PLoS ONE 2016;11:e0168904.

46 Zhu L, Gibson P, Currle DS et al. Prominin1/CD133 marks intestinal stem cells that are susceptible to neoplastic transformation. Nature 2009;457:603–607.

47 Barker N, Huch M, Kujala P et al. Lgr5 (+ve) stem cells drive self-renewal in the stomach and build long-lived gastric units in vitro. Cell Stem Cell 2010;6:25–36.

48 Wen L, Chen XZ, Yang K et al. Prognostic value of cancer stem cell marker CD133 expression in gastric cancer: A systematic review. PLoS One 2013;8(3):e59154.

49 Zhao Y, Feng F, Zhou YN. Stem cells in gastric cancer. World J Gastroenterol 2015;21: 112–123.

50 Sahlberg SH, Spiegelberg D, Glimelius B et al. Evaluation of cancer stem cell markers CD133, CD44, CD24: Association with AKT isoforms and radiation resistance in colon cancer cells. PLoS ONE 2014;9:e94621.

51 Carmon KS, Gong X, Lin QS et al. R-spondins function as ligands of the orphan receptors LGR4 and LGR5 to regulate Wnt/-beta-catenin signaling. Proc Natl Acad Sci USA 2011;108:11452–11457.

52 Hao HX, Xie Y, Zhang Y et al. ZNRF3 promotes Wnt receptor turnover in an R-spondin-sensitive manner. Nature 2012; 485:195–200.

53 Koo BK, Spit M, Jordens I et al. Tumour suppressor RNF43 is a stem-cell E3 ligase that induces endocytosis of Wnt receptors. Nature 2012;488:665–669.

54 Clevers H, Loh KM, Nusse R. Stem cell signaling. An integral program for tissue renewal and regeneration: Wnt signaling and stem cell control. Science 2014;346:1248012.

55 Novellasdemunt L, Antas P, Li VSW. Targeting Wnt signaling in colorectal cancer. A review in the theme: Cell signaling: Proteins, pathways and mechanisms. Am J Physiol Cell Physiol 2015;309:C511–C521.

56 Nusse R, Clevers H. Wnt/beta-catenin signaling, disease, and emerging therapeutic modalities. Cell 2017;169:985–999.

57 Zhan T, Rindtorff N, Boutros M. Wnt signaling in cancer. Oncogene 2017;36:1461–1473.

58 Fuerer C, Nusse R. Lentiviral vectors to probe and manipulate the Wnt signaling pathway. PLoS ONE 2010;5:e9370.

59 Dawood S, Austin L, Cristofanilli M. Cancer stem cells: Implications for cancer therapy. Oncology 2014;28:1101.

60 Harris TJ, Peifer M. Decisions, decisions: Beta-catenin chooses between adhesion and transcription. Trends Cell Biol 2005;15: 234–237.

61 MacDonald BT, Tamai K, He X. Wnt/beta-catenin signaling: Components, mechanisms, and diseases. Dev Cell 2009;17:9–26.

62 Lien WH, Fuchs E. Wnt some lose some: Transcriptional governance of stem cells by Wnt/beta-catenin signaling. Genes Dev 2014; 28:1517–1532.

63 Vermeulen L, Melo FDSE, van der Heijden M et al. Wnt activity defines colon cancer stem cells and is regulated by the microenvironment. Nat Cell Biol 2010;12: 468–476.

64 Eyre R, Harvey I, Stemke-Hale K et al. Reversing paclitaxel resistance in ovarian cancer cells via inhibition of the ABCB1 expressing side population. Tumour Biol 2014;35: 9879–9892.

See www.StemCells.com for supporting information available online.